

Qualitative and quantitative features of orbits of massive particles and photons moving in Wyman geometry.

G Oliveira-Neto¹ and G F Sousa²

¹ Departamento de Matemática e Computação, Faculdade de Tecnologia, Universidade do Estado do Rio de Janeiro, Rodovia Presidente Dutra Km 298, Pólo Industrial, CEP 27537-000, Resende-RJ, Brazil.

² Departamento de Física, Instituto de Ciências Exatas, Universidade Federal de Juiz de Fora, CEP 36036-330, Juiz de Fora, Minas Gerais, Brazil.

E-mail: gilneto@fat.uerj.br, gilberto_freitas@yahoo.com.br

Abstract. The Wyman's solution depends on two parameters, the mass M and the scalar charge σ . If one fixes M to a positive value, say M_0 , and let σ^2 take values along the real line it describes three different types of spacetimes. For $\sigma^2 > 0$ the spacetimes are naked singularities, for $\sigma^2 = 0$ one has the Schwarzschild black hole of mass M_0 and finally for $-M_0^2 \leq \sigma^2 < 0$ one has wormhole spacetimes. In the present work, we shall study qualitative and quantitative features of orbits of massive particles and photons moving in the naked singularity and wormhole spacetimes of the Wyman solution. These orbits are the timelike geodesics for massive particles and null geodesics for photons. Combining the four geodesic equations with an additional equation derived from the line element, we obtain an effective potential for the massive particles and a different effective potential for the photons. We investigate all possible types of orbits, for massive particles and photons, by studying the appropriate effective potential. We notice that for certain values of $\sigma^2 > 0$, there is an infinity potential wall that prevents both massive particles and photons ever to reach the naked singularity. We notice, also, that for certain values of $-M_0^2 \leq \sigma^2 < 0$, the potential is finite everywhere, which allows massive particles and photons moving from one wormhole asymptotically flat region to the other. We also compute the radial timelike and null geodesics for massive particles and photons, respectively, moving in the naked singularities and wormholes spacetimes.

PACS numbers: 04.20.Dw, 04.20.Jb, 04.40.Nr, 04.70.Bw

Submitted to: *Class. Quantum Grav.*

1. Introduction

The *weak equivalence principle* of general relativity tell us that massive particles move along timelike geodesics and photons move along null geodesics [1]. Despite their fundamental importance as one of the principles of general relativity, the geodesics also help us learning more about different properties of a given spacetime. A textbook example comes from the study of geodesics in Schwarzschild geometry [1]. Without actually computing the geodesics, just observing the effective potential diagram, one can see that both massive particles and photons can never leave the event horizon once they enter that surface. This is the case because the effective potential for both massive particles and photons diverges to negative infinity as one approaches the singularity located at the coordinate system origin. Therefore, once the massive particles and photons enter the event horizon they are accelerated toward the singularity without any chance to turn back. Many authors, over the years, have computed the effective potential diagram and the geodesics of different spacetimes in order to learn more about their properties. In particular, we may mention some important works dealing with different black hole spacetimes [2]. Two other important gravitational configurations besides black holes that may form due to the gravitational collapse are naked singularities and wormholes. Some authors have already investigated some of their properties by computing effective potential diagrams and geodesics for those space-times [3, 4, 5]. A well-known spacetime geometry which may describe naked singularities as well as wormholes is the Wyman one [6]. Since, to the best of our knowledge, nobody has ever studied the Wyman spacetime by means of the computation of its effective potential diagrams and geodesics, we decided to do that in the present work.

The Wyman geometry describes the four dimensional space-time generated by a minimally coupled, spherically symmetric, static, massless scalar field and has been studied by many authors [6, 7, 8, 9, 10, 11]. From a particular case of the general Wyman's solution, M. D. Roberts showed how to construct a time dependent solution [8]. The Roberts' solution has an important physical interest because it may represent the gravitational collapse of a scalar field. Later, P. Brady and independently Y. Oshiro et al. [12], [13] showed that the Roberts' solution could be derived from the appropriated, time-dependent, Einstein-scalar equations by using a continuous self-similarity. They also showed that the Roberts' solution exhibits a critical behavior qualitatively identical to the one found numerically by M. W. Choptuik [14], studying the same system of equations. In fact, the above results confirmed early studies of D. Christodoulou who pioneered analytical studies of that model [15].

The Wyman's solution is not usually thought to be of great importance for the issue of gravitational collapse because it is static and the naked singularities derived from it are unstable against spherically symmetric linear perturbations of the system [9, 10]. On the other hand, as we saw above, from a particular case of the Wyman's solution one may derive the Roberts' one which is of great importance for the issue of gravitational collapse. Also, it was shown that there are nakedly singular solutions to

the static, massive scalar field equations which are stable against spherically symmetric linear perturbations [10]. Therefore, we think it is of great importance to gather as much information as we can about the Wyman's solution for they may be helpful for a better understand of the scalar field collapse.

The Wyman's solution depends on two parameters, the mass M and the scalar charge σ . If one fixes M to a positive value, say M_0 , and let σ^2 take values along the real line it describes three different types of spacetimes. For $\sigma^2 > 0$ the spacetimes are naked singularities, for $\sigma^2 = 0$ one has the Schwarzschild black hole of mass M_0 and finally for $-M_0^2 \leq \sigma^2 < 0$ one has wormhole spacetimes. Therefore, we have an interesting situation where we can study different properties of naked singularities and wormholes together through the effective potential diagrams and geodesics of massive particles and photons in the Wyman's solution.

In the next Section, we introduce the Wyman solution and identify the values of the parameters M and η that describes naked singularities, wormholes and the Schwarzschild black hole. In Section 3, we combine the geodesic equations to obtain the effective potential equation for the case of massive particles. We study the effective potential and qualitatively describe the types of orbits for massive particles moving in the naked singularities and wormholes spacetimes. In this section, we also compute the radial timelike geodesics for particles moving in the naked singularities and wormholes spacetimes. In Section 4, we combine the geodesic equations to obtain the effective potential equation for the case of photons. We study the effective potential and qualitatively describe the types of orbits for photons moving in the naked singularities and wormholes spacetimes. In this section, we also compute the radial timelike geodesics for photons moving in the naked singularities and wormholes spacetimes. Finally, in Section 5 we summarize the main points and results of our paper.

2. Naked singularities, wormholes and the Schwarzschild black hole.

The Wyman line element and the scalar field expression are given in terms of the coordinates (t, r, θ, ϕ) by the equation (9) of [8],

$$ds^2 = -\left(1 - \frac{2\eta}{r}\right)^{\frac{M}{\eta}} dt^2 + \left(1 - \frac{2\eta}{r}\right)^{-\frac{M}{\eta}} dr^2 + \left(1 - \frac{2\eta}{r}\right)^{1-\frac{M}{\eta}} r^2 d\Omega^2, \quad (1)$$

where r varies in the range $2\eta < r < \infty$ and $d\Omega^2$ is the line element of the two-dimensional sphere with unitary radius. The scalar field is,

$$\varphi = \frac{\sigma}{2\eta} \ln \left(1 - \frac{2\eta}{r}\right). \quad (2)$$

where σ is the scalar charge given by $\sigma^2 = \eta^2 - M^2$ and $\sigma^2 \geq -M^2$. We are working in the unit system where $G = c = 1$.

In the line element (1), the function $R(r)$,

$$R(r) = r \left(1 - \frac{2\eta}{r}\right)^{\frac{1}{2}(1-\frac{M}{\eta})}, \quad (3)$$

is the physical radius which gives the circumference and area of the two-spheres present in the Wyman geometry. Instead of using the parameters M and σ to identify the different types of spacetimes described by (1), we may also use the parameters M and η , since they are all related by the equation just below (2). Each different type of spacetime will have a different behaviour of the function $R(r)$. $R(r)$ has a single extreme point which is a minimum located at $r = M + \eta$. Since, the line element (1) is valid for $r > 2\eta$, only in the cases where $M > \eta$ there will be a minimum inside the domain of r . Based on that result we have three different cases for a positive M . As a matter of simplicity we shall use, also, the positive parameter $\lambda \equiv M/\eta$ in order to identify the three different cases.

Case $M < \eta$ or $0 < \lambda < 1$.

In this case we have the following important values of $R(r)$ (3),

$$\lim_{r \rightarrow 2\eta_+} R(r) = 0, \quad \lim_{r \rightarrow \infty} R(r) = \infty. \quad (4)$$

Here, the solution represents space-times with a physical naked timelike singularity located at $R = 0$ [7]. It is easy to see that this singularity is physical because, the Ricci scalar \mathbf{R} computed from the line element (1),

$$\mathbf{R} = \frac{2(M^2 - \eta^2)}{r^4} \left(1 - \frac{2\eta}{r}\right)^{\frac{M}{\eta} - 2}, \quad (5)$$

diverges there. It is also easy to see that this singularity is naked with the aid of the quantity $Q = g^{\alpha\beta} \frac{\partial R}{\partial x^\alpha} \frac{\partial R}{\partial x^\beta}$. The roots of Q determine the presence of event horizons in spherical symmetric spacetimes [12]. For the Wyman solution Q is given by,

$$Q = \left(1 - \frac{2\eta}{r}\right)^{-1} \left(1 - \frac{M + \eta}{r}\right)^2. \quad (6)$$

The only root of Q is located at $r = M + \eta$ which confirms that the singularity located at $R = 0$ is naked for all spacetimes in the present case.

This singularity is sometimes called a ‘central singularity’ and is similar to that appearing in the ‘extreme’ Reissner-Nordström black hole and in the negative mass Schwarzschild spacetime. From equation (2), the scalar field vanishes asymptotically as $R \rightarrow \infty$ and diverges at the singularity.

Case $M = \eta$ or $\lambda = 1$.

In this case we have $R(r) = r$ and $\sigma = 0$. This last condition implies that the scalar field (2) vanishes and one gets the Schwarzschild solution. Here, the minimum of $R(r)$, located at $R = 2M$, is outside the domain of r and the line element (1) describes only the spacetime exterior to the event horizon.

Case $M > \eta$ or $1 < \lambda < \infty$.

In this case we have the following important values of $R(r)$ (3),

$$\lim_{r \rightarrow 2\eta_+} R(r) = \infty, \quad R_{min} = (M + \eta) \left(\frac{M - \eta}{M + \eta}\right)^{\frac{1}{2}(1 - \frac{M}{\eta})}, \quad \lim_{r \rightarrow \infty} R(r) = \infty. \quad (7)$$

Due to the fact that $\sigma^2 \geq -M^2$ as stated just before (2), we have that in the present case $\eta \geq 0$. The case $\eta = 0$ is well known in the literature as the Yilmaz-Rosen space-time

[16]. In this case $M > \eta$, the physical radius R is never zero. If one starts with a large value of R , for large values of r , and starts diminishing R , reducing the values of r , one will reach the minimum value of R (R_{min} (7)) for $r = M + \eta$. Then, R starts to increase again when we let r goes to 2η until it diverges when $r = 2\eta$. Therefore, we may interpret these spacetimes as wormholes connecting two asymptotically flat regions such that they have a minimum throat radius given by R_{min} (7) [11]. The spatial infinity ($R \rightarrow \infty$) of each asymptotically flat region is obtained, respectively, by the limits: $r \rightarrow \infty$ and $r \rightarrow 2\eta_+$. An important property of this space-time is that the scalar field (2) is imaginary. The imaginary scalar field also known as ghost Klein-Gordon field [17] is an example of the type of matter called *exotic* by some authors [18]. It violates most of the energy conditions and is repulsive. This property helps explaining the reason why the collapsing scalar field never reaches $R = 0$.

As mentioned above, in the rest of the paper we shall restrict our attention to the spacetimes representing naked singularities and wormholes.

3. Timelike Geodesics

3.1. Effective Potential

We have four geodesic equations, one for each coordinate [1],

$$\frac{d^2 x^\alpha}{d\tau^2} + \Gamma_{\beta\gamma}^\alpha \frac{dx^\beta}{d\tau} \frac{dx^\gamma}{d\tau} = 0, \quad (8)$$

where $\alpha = 0, 1, 2, 3$, and x^α represents, respectively, each of the coordinates (t, r, θ, ϕ) . τ is the proper time of the massive particle which trajectory is described by (8).

The geodesic equation in the coordinate θ tell us that, like in the Schwarzschild case, the geodesics are independent of θ , therefore we choose the equatorial plane to describe the particle motion ($\theta = \pi/2$). In the equatorial plane, the geodesic equation for ϕ may be once integrate to give,

$$r^2 \left(1 - \frac{2\eta}{r}\right)^{1-\frac{M}{\eta}} \dot{\phi} = R^2 \dot{\phi} = L, \quad (9)$$

where the dot means derivative with respect to τ and L is the integration constant that may be interpreted as the particle angular momentum per unit rest mass. This result means that ϕ is *cyclic* and its conjugated momentum ($p_\phi = \dot{\phi}$) is a conserved quantity. Also, $\dot{\phi}$ may be written as a function of r . Likewise, in the equatorial plane, the geodesic equation for t may be once integrate to give,

$$\left(1 - \frac{2\eta}{r}\right)^{\frac{M}{\eta}} \dot{t} = E, \quad (10)$$

where E is the integration constant that may be interpreted as the particle energy per unit rest mass. This result means that t is *cyclic* and its conjugated momentum ($p_t = \dot{t}$) is a conserved quantity. Also, \dot{t} may be written as a function of r . Instead of using the fourth geodesic equation for the r coordinate, we use the equation derived directly from

the line element (1), $ds^2/d\tau^2 = -1$ [19]. There, we introduce the expressions of $\dot{\phi}$ (9) and \dot{t} (10), in order to obtain the following equation which depends only on r ,

$$\left(\frac{dr}{d\tau}\right)^2 + V(r)^2 = E^2. \quad (11)$$

Where

$$V(r)^2 = \left(1 - \frac{2\eta}{r}\right)^{\frac{M}{\eta}} \left[1 + \frac{L^2}{r^2} \left(1 - \frac{2\eta}{r}\right)^{\frac{M}{\eta}-1}\right] \quad (12)$$

and $V(r)$ is the effective potential for the motion of massive particles in the Wyman geometry. The geodesic equation for the r coordinate plays the role of a control equation, where we substitute the solutions found with the other four equations in order to verify their correctness.

In order to have a qualitative idea on the orbits of massive particles moving under the action of $V(r)^2$ it is important to draw it as a function of r . We may do it by, initially, computing the extremes of $V(r)^2$. First, we calculate the first derivative of $V(r)^2$ (12) and find the roots of the resulting equation. That equation may be simplified by the introduction of the auxiliary quantities: $x = (1 - 2\eta/r)$, $0 < x < 1$; $A = \eta^2/L^2$, $0 < A < \infty$; $B = (\lambda - 1/2)/(\lambda + 1/2)$, $-1 < B < 1$; $C = 2\lambda/(\lambda + 1/2)$, $0 < C < 2$. Where λ was defined before and the domains of A , B and C were determined by the fact that λ is positive. The equation $dV(r)/dr = 0$, in terms of x , λ , A , B and C is given by,

$$ACx^{1-\lambda} + B - Cx + x^2 = 0. \quad (13)$$

In order to identify the presence and nature of the roots of (13), let us define the following two auxiliary functions,

$$p(x) = -x^2 + Cx - B, \quad h(x) = ACx^{1-\lambda}. \quad (14)$$

Now, the values of x where the two curves $p(x)$ and $h(x)$ meet will be the roots of (13). $p(x)$ is a set of parabolas which vertices are all located above the x-axis and with two roots. The larger one is located at $x = 1$ and the smaller one is located at $x = (\lambda - 1/2)/(\lambda + 1/2)$. For $\lambda > 1/2$, the smaller root is positive; for $\lambda = 1/2$, it is zero and for $\lambda < 1/2$, it is negative. The precise nature of $h(x)$ will depend on the value of λ , present in the exponent of x , but whatever λ one chooses, all values of $h(x)$ will be located above the x-axis. For $\lambda > 1$, $h(x)$ diverges to $+\infty$ when $x \rightarrow 0$ and goes to zero when $x \rightarrow +\infty$. For $\lambda < 1$, $h(x)$ goes to zero when $x \rightarrow 0$ and diverges to $+\infty$ when $x \rightarrow +\infty$.

An important root of (13) is defined by the value of x , say x_0 , where the two curves $p(x)$ and $h(x)$ (14) just touch each other. x_0 is an inflection point of $V(r)^2$ (12), because there the second derivative of $V(r)^2$ is also zero. Associated to x_0 there is a value of the angular momentum L , say L_0 , which originates an unstable particle orbit. Due to the fact that L is present, only, in the denominator of A in the expression of $h(x)$ (14), if one increases L , $h(x)$ will assume smaller values for the same values of x . $p(x)$ will not

be altered because L is not present in its expression. Therefore, L_0 is the value of L for which $h(x)$ just touches $p(x)$, if one takes values of L greater than L_0 , $h(x)$ will start intercepting $p(x)$ in two or more points. They will be extremes of $V(r)^2$, maximum, minimum or inflection points. It is possible to compute the value of L_0 in terms of x_0 and the parameters λ and η . In order to do that, we consider, initially, the fact that the first derivatives of $h(x)$ and $p(x)$ (14), in $x = x_0$, are equal and express $ACx_0^{-\lambda}$ in terms of other quantities. Then, we use the fact that x_0 is a root of (13) and re-write that equation for $x = x_0$ and substitute there the value of $ACx_0^{-\lambda}$ just obtained. It gives rise to the following second degree polynomial equation in x_0 ,

$$x_0^2 - \frac{C\lambda}{\lambda+1}x_0 + \frac{\lambda-1}{\lambda+1}B = 0, \quad (15)$$

where $\lambda \neq 1$. It has the following roots,

$$x_0^+ = \frac{2\lambda^2 + \sqrt{5\lambda^2 - 1}}{2(\lambda + 1/2)(\lambda + 1)}, \quad x_0^- = \frac{2\lambda^2 - \sqrt{5\lambda^2 - 1}}{2(\lambda + 1/2)(\lambda + 1)}, \quad (16)$$

where $x_0^+ \geq x_0^-$. Due to the fact that we have two distinct values of x_0 , x_0^+ and x_0^- given by (16), we shall have, also, two distinct values of L_0 , say L_{0+} and L_{0-} . In order to obtain them, we introduce x_0^+ and x_0^- , separately, in the equation that equates the first derivatives of $h(x)$ and $p(x)$ and express L_0^2 in term of other quantities. It results in,

$$L_{0+}^2 = \frac{\eta^2\lambda(1-\lambda)}{(x_0^+)^{\lambda}[\lambda - x_0^+(\lambda + 1/2)]}, \quad L_{0-}^2 = \frac{\eta^2\lambda(1-\lambda)}{(x_0^-)^{\lambda}[\lambda - x_0^-(\lambda + 1/2)]}, \quad (17)$$

where $L_{0-}^2 \geq L_{0+}^2$.

By definition λ has the domain $[0, \infty)$, but if one introduces values of λ , over all this domain, in the expressions of x_0^+ , x_0^- (16) and L_{0+}^2 , L_{0-}^2 (17), one will find some unphysical results. This means that one will have to impose some restrictions on the domain of λ . These restrictions will have to take in account the following two conditions: (i) x_0^+ and x_0^- varies in the range $[0, 1]$, due to the definition of x ; (ii) L_{0+}^2 and L_{0-}^2 must be positive. These conditions lead to the following distinct domains of λ , depending on the extreme x_0^+ or x_0^- one is using,

$$x_0^- : \quad \frac{1}{\sqrt{5}} \leq \lambda < \frac{1}{2}, \quad (18)$$

$$x_0^+ : \quad \lambda \geq \frac{1}{\sqrt{5}}. \quad (19)$$

Therefore, this result tell us that $V(r)^2$ (12) behaves differently, depending on the value of λ . We have the following three different regions:

(i) $\lambda \geq 1/2$.

There will be just one inflection point located at x_0^+ for L_{0+}^2 . If one chooses values of $L^2 > L_{0+}^2$, one will find other extremes of $V(r)^2$ (12), which will be maximum or minimum points.

(ii) $1/\sqrt{5} \leq \lambda < 1/2$.

There may be two different inflection points. The first located at x_0^+ for $L^2 = L_{0+}^2$. If one chooses values of $L^2 > L_{0+}^2$, one will find other extremes of $V(r)^2$ (12), which will be maximum or minimum points. When one reaches $L^2 = L_{0-}^2$, one finds the other possible inflection point located at x_0^- . If one chooses values of $L^2 > L_{0-}^2$, one will find just one extreme of $V(r)^2$ (12), which will be a minimum point. Even for the case $L^2 < L_{0+}^2$, there will be a minimum point. In fact, this minimum point will always be present for any value of L . Its presence can be understood because, here, $p(x)$ has a negative root and $h(x)$ is crescent and starts from $x = 0$. Therefore, these two curves will always intercept each other.

(iii) $\lambda < 1/\sqrt{5}$.

There will be no inflection points but there will be always a minimum point. The presence of this minimum point can be understood in the same way as the one in the previous case.

As we saw in the previous section, Sec. 2, naked singularities and wormholes are characterized by certain subdomains of λ . Therefore, based on the above result, we may draw the effective potentials for naked singularities and wormholes. From these effective potentials, we shall be able to describe qualitatively the different orbits of massive particles.

3.2. Effective Potential for Naked Singularities

As we saw, in Sec. 2, the naked singularities are obtained for $0 < \lambda < 1$. We may still divide the naked singularities in two classes, due to the behavior of $V(r)^2$ (12) when $r \rightarrow 2\eta_+$. For $0 < \lambda < 1/2$, $V(r)^2$ (12) assumes the following values when $r \rightarrow 2\eta_+$ and $r \rightarrow +\infty$,

$$\lim_{r \rightarrow 2\eta_+} V(r)^2 = \infty, \quad \lim_{r \rightarrow +\infty} V(r)^2 = 1. \quad (20)$$

Due to the fact that these limits are consistent with an asymptotically flat naked singularity located at $r = 2\eta$, we call this class of ordinary naked singularities. On the other hand, for $1/2 \leq \lambda < 1$ the limit of $V(r)^2$ (12) when $r \rightarrow 2\eta_+$ is zero. Due to fact that this result is not consistent with a naked singularity located at $r \rightarrow 2\eta$, we call this class of *anomalous naked singularities*. Then, in what follows we shall restrict our attention to the class of ordinary naked singularities with $0 < \lambda < 1/2$. It is important to mention that observing the scalar field expression (2), which in this case is real, one can see that it diverges to $-\infty$ as $r \rightarrow 2\eta_+$.

Taking in account the results of Subsec. 3.1 (ii) and (iii) the effective potential $V(r)^2$ (12) may have several different shapes depending on the value of L^2 . Here, the inflection points will be located at x_0^- and x_0^+ (16) and the relevant angular momenta will be L_{0-}^2 and L_{0+}^2 (17).

- For $L^2 < L_{0+}^2$, $V(r)^2$ (12) has one minimum point. In terms of x it is located in the range $(0, x_0^-)$ or in terms of r it is located in the range $(2\eta, r_0^- \equiv 2\eta/(1 - x_0^-))$. For $E^2 < 1$, the massive particles orbit around the naked singularity. If the massive

particle is located exactly at the minimum point the orbit is circular and stable. For $E^2 > 1$, the massive particles come in from infinity reach the infinity potential wall near the naked singularity and return to infinity without ever reach the naked singularity.

- For $L^2 = L_{0+}^2$, $V(r)^2$ (12) has two extreme points, a minimum located in the range $(2\eta, r_0^-)$ and an inflection point located at $r = r_0^+ \equiv 2\eta/(1 - x_0^+)$. In this point the massive particles have unstable circular orbits. The other possible trajectories for the massive particles are exactly as in the previous case.
- For $L_{0+}^2 < L^2 < L_{0-}^2$, $V(r)^2$ (12) has three extreme points, a minimum located in the range $(2\eta, r_0^-)$, a maximum located in the range (r_0^-, r_0^+) and another maximum located in the range (r_0^+, ∞) . If the massive particles are exactly in the maximum points they have unstable circular orbits. The other possible trajectories for the massive particles are exactly as in the first case.
- For $L^2 = L_{0-}^2$, $V(r)^2$ (12) has two extreme points, a minimum located in the range (r_0^+, ∞) and an inflection point located at $r = r_0^-$. In this point the massive particles have unstable circular orbits. The other possible trajectories for the massive particles are exactly as in the first case.
- For $L^2 > L_{0-}^2$, $V(r)^2$ (12) has one minimum point located in the range (r_0^+, ∞) . The possible trajectories for the massive particles are exactly as in the first case.

It is important to mention that, for sufficiently large values of E , any massive particles will come in from infinity and it will get reflected by the infinity potential wall near the naked singularity. Then, it will return to infinity without ever reach the naked singularity. This result is similar to the one found in [4] for timelike geodesics of the naked singularity present in the Reissner-Nordström spacetime. Let us consider, as an example, the case where $M = 10$ and $\lambda = 0.45$. Therefore, we have $L_{0+}^2 = 954.9308516$ and $x_0^+ = 0.1875874406$ which in terms of r is given by $r_0^+ = 54.70674220$. We also have, $L_{0-}^2 = 960.0309665$ and $x_0^- = 0.1064234487$ which in terms of r is given by $r_0^- = 49.73770224$. In the Figure 1, we plot five different effective potential diagrams from $V(r)^2$ (12), one for each of the five cases discussed above. They have the five different values of L^2 : 951, 954.9308516, 957, 960.0309665 and 962. The naked singularity is located at $r = 44.44444444$.

3.3. Effective Potential for Wormholes

As we saw, in Sec. 2, the wormholes are obtained for $1 < \lambda < \infty$. In the spatial infinity of each asymptotically flat region the effective potential $V(r)^2$ (12) assumes the following values,

$$\lim_{r \rightarrow 2\eta_+} V(r)^2 = 0, \quad \lim_{r \rightarrow \infty} V(r)^2 = 1. \quad (21)$$

Although the above limits give consistent values for the effective potential at the two spatial infinities, the first limit is not consistent with the value of the Ricci scalar

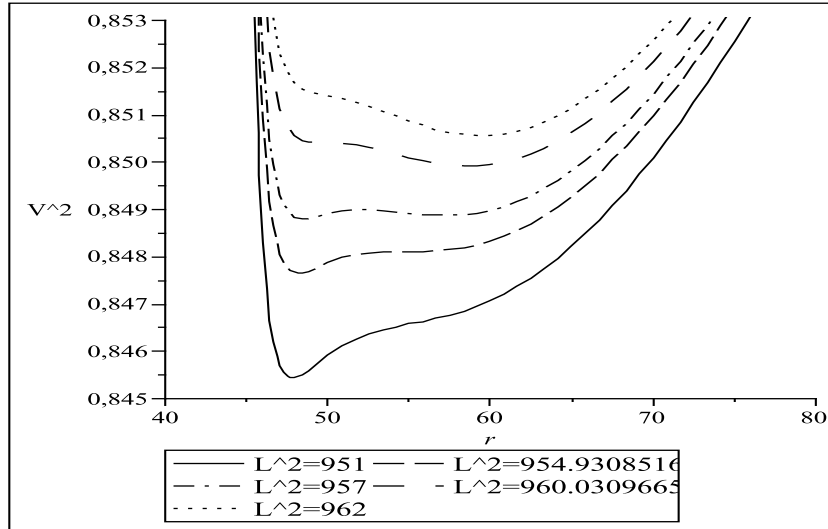


Figure 1. Five different effective potential diagrams from $V(r)^2$ (12), for massive particles moving in a naked singularity with $M = 10$ and $\lambda = 0.45$. They have the five different values of L^2 : 951, 954.9308516, 957, 960.0309665 and 962. The naked singularity is located at $r = 44.44444444$.

evaluated at $r = 2\eta$, for wormholes with $1 < \lambda \leq 2$. For this class of wormholes the Ricci scalar \mathbf{R} (5), diverges to ∞ when we take the limit $r \rightarrow 2\eta_+$ or gives a positive constant when $\lambda = 2$. These values are not consistent with the first limit of $V(r)^2$ in (21) and the idea of an asymptotically flat spatial region. Therefore we call this class of wormholes of *anomalous wormholes*. For the rest of the wormholes where $2 < \lambda < \infty$, the limit of \mathbf{R} (5) when $r \rightarrow 2\eta_+$ is zero. This value is consistent with the first limit of $V(r)^2$ in (21) and the idea of an asymptotically flat spatial region. Then, in what follows we shall restrict our attention to that class of ordinary wormholes with $2 < \lambda < \infty$. It is important to mention that observing the scalar field expression (2), which in this case is imaginary, one can see that it diverges to $-\infty$ as $r \rightarrow 2\eta_+$. Since there is no physical singularity at $r \rightarrow 2\eta_+$ for the ordinary class of wormholes, this result indicates that the coordinates we are using might not be suitable to describe this asymptotically flat region.

Taking in account the results of Subsec. 3.1 (i) the effective potential $V(r)^2$ (12) may have three different shapes depending on the value of L^2 . Here, the inflection point will be located at x_0^+ (16) and the relevant angular momentum will be L_{0+}^2 (17).

- For $L^2 < L_{0+}^2$, $V(r)^2$ (12) has no extreme points. In this case, there is no stable orbits. For sufficiently high energies the massive particles may travel from one asymptotically flat region to the other. In fact, this type of orbit is also present in the other two cases considered below.
- For $L^2 = L_{0+}^2$, $V(r)^2$ (12) has one inflection point, located at x_0^+ (16) or in terms of r , $r_0^+ \equiv 2\eta/(1 - x_0^+)$. In this point the massive particles have unstable circular orbits.

- For $L^2 > L_{0+}^2$, $V(r)^2$ (12) has two extreme points, a maximum located at $2\eta < r < r_0^+$ and a minimum located at $r_0^+ < r$. There are closed and open orbits depending on the values of the total energy and angular momentum of the massive particles.

Let us consider, as an example, the case where $M = 1$ and $\lambda = \sqrt{1000}$. Therefore, we have $L_{0+}^2 = 12.41266$ and $x_0^+ = 0.98799$ which in terms of r is given by $r_0^+ = 5.26747$. In the Figure 2, we plot three different effective potential diagrams from $V(r)^2$ (12), one for each of the three cases discussed above. They have the three different values of L^2 : 10, 12.41266 and 14.4. The spatial infinities of each asymptotically flat region are located at $r = 0.06325$ and $r \rightarrow \infty$.

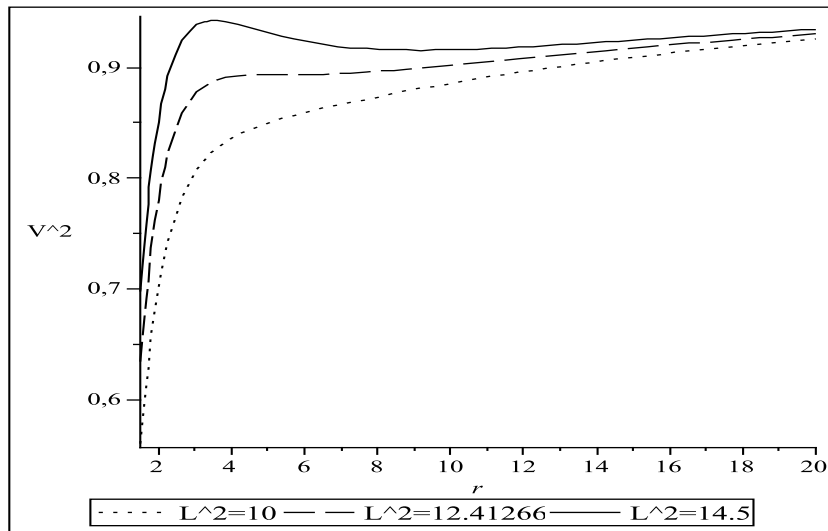


Figure 2. Three different effective potential diagrams from $V(r)^2$ (12), for massive particles moving in a wormhole with $M = 1$ and $\lambda = \sqrt{1000}$. They have the three different values of L^2 : 10, 12.41266 and 14.4. The spatial infinities of each asymptotically flat region are located at $r = 0.06325$ and $r \rightarrow \infty$.

It is important to mention, at this point, that the same study of the qualitative features of the orbits of massive particles in Wyman geometry in terms of the proper time τ , as we just did, can also be done in terms of the coordinate time t . In order to do it, we re-write equation (11) in the following way,

$$\left(E \frac{dr^*}{dt}\right)^2 + V(r)^2 = E^2, \quad (22)$$

where we used the relationship, $dt/d\tau = E/(1 - 2\eta/r)^\lambda$, and we introduced the generalization of the Wheeler's *tortoise coordinate* r^* [1], given by,

$$r^* = \int \frac{dr}{\left(1 - \frac{2\eta}{r}\right)^\lambda}. \quad (23)$$

Since, $V(r)$ and E in (22) are the same as the ones in (11), the turning points of $V(r)$, for a given value of E , are the same whether we use t or τ . On the other hand, the geodesics may have different properties depending on the time variable we are using. We shall see some similarities and differences in the next section.

3.4. Radial timelike geodesics

3.4.1. Description in terms of τ Unfortunately, there is not an analytic expression for the general timelike geodesics given by the solutions of Eqs. (9-11), even the numerical solutions are very complicated. On the other hand, one may restrict his attention to the case of radial timelike geodesics, where the massive particle moves only along the radial and time directions. It means that $\dot{\theta} = \dot{\phi} = L = 0$ and (11) reduces to,

$$\left(\frac{dr}{d\tau}\right)^2 = E^2 - \left(1 - \frac{2\eta}{r}\right)^{\frac{M}{\eta}}. \quad (24)$$

Although (24) is much simpler than (11), one still cannot integrate it to find an analytic expression of τ as a function of r . The best one can do is finding a numerical solution for the integral and plot that solution in a graph of τ versus r . We did that and we shall present the results below, for the naked singularities and wormholes.

Naked singularities In this case, we integrated (24) for many different values of E , M and η . We chose values of M and η compatibles with naked singularities. We found that, for $E \geq 1$, the geodesics are all well behaved when $r \rightarrow 2\eta$. In fact, τ goes to zero in that limit. The geodesics are such that when r is large, r tends to a linear function of the proper time τ . For $E < 1$, the geodesics are also well behaved when $r \rightarrow 2\eta$ and τ also goes to zero in that limit. On the other hand, they do not extend to large values of r . It is clear from (24), that the massive particle is subjected to a potential of the form: $(1 - 2\eta/r)^{M/\eta}$. This potential, increases from zero at $r = 2\eta$ and tends to one when $r \rightarrow \infty$. Therefore, massive particles with a total energy $E < 1$, get reflected by the potential. The value of r , where the particle gets reflected by the potential is obtained by solving the equation: $E^2 = (1 - 2\eta/r)^{M/\eta}$. Then, based on the above results, we may conclude that it always takes a finite proper time interval to travel from any finite value of r to the singularity located at $r = 2\eta$. We notice, also, that for radial timelike geodesics there is not an infinity potential wall near the naked singularity and the massive particles can reach it. In the Figure 3, we show as an example a geodesic for the case: $E = 1$, $M = 1$ and $\eta = 3$. The naked singularity is located at $r = 6$ and the geodesics extends to large values of r . In the Figure 4, we show as an example a geodesic for the case: $E = 0.5$, $M = 1$ and $\eta = 3$. The naked singularity is located at $r = 6$ and the geodesics gets reflected at $r = 6.095238095$. One cannot see the geodesic returning to $r = 6$, from this figure, because we have considered only the outgoing geodesic.

Wormholes In this case, we integrated (24) for many different values of E , M and η . We chose values of M and η compatibles with wormholes. We found that, for $E \geq 1$, the

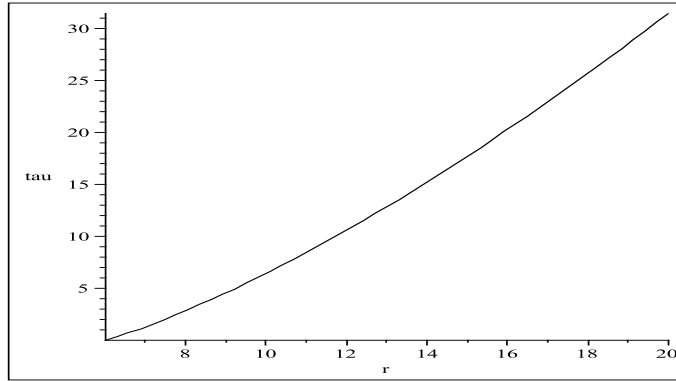


Figure 3. Radial geodesic, described in terms of τ , for a massive particle moving in a naked singularity with $E = 1$, $M = 1$ and $\eta = 3$. The naked singularity is located at $r = 6$.

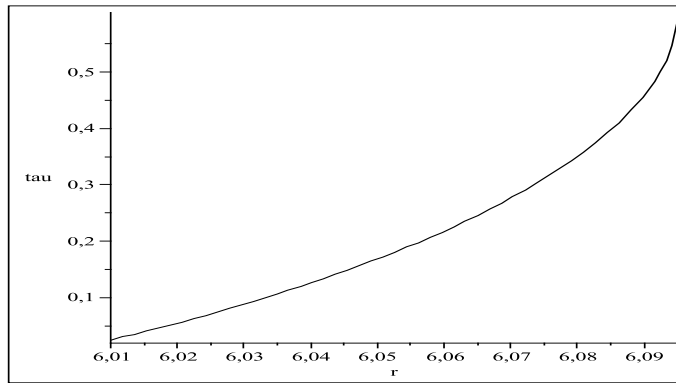


Figure 4. Radial geodesic, described in terms of τ , for a massive particle moving in a naked singularity with $E = 0.5$, $M = 1$ and $\eta = 3$. The naked singularity is located at $r = 6$.

geodesics are all well behaved when $r \rightarrow 2\eta$. In fact, τ goes to zero in that limit. The geodesics are such that when r is large, r tends to a linear function of the proper time τ . For $E < 1$, the geodesics are also well behaved when $r \rightarrow 2\eta$ and τ also goes to zero in that limit. On the other hand, they do not extend to large values of r because they get reflected by the potential, as in the naked singularity case. The value of r , where the particle gets reflected by the potential is obtained in the same way we proceeded in the naked singularity case. Here, as in the naked singularity case, for all cases studied it always takes a finite proper time interval to travel from any finite value of r to the spatial infinity located at $r = 2\eta$. In the Figure 5, we show as an example a geodesic for the case: $E = 1$, $M = 3$ and $\eta = 1$. The spatial infinities of each asymptotically flat regions are located at $r = 2$ and $r \rightarrow \infty$ and the geodesics extends to large values of r .

3.4.2. Description in terms of t Here, as in the case where the geodesics are described in terms of τ , the treatment of the general situation is very complicated. Therefore, we shall, also, restrict our attention to the particular situation of radial timelike geodesics.

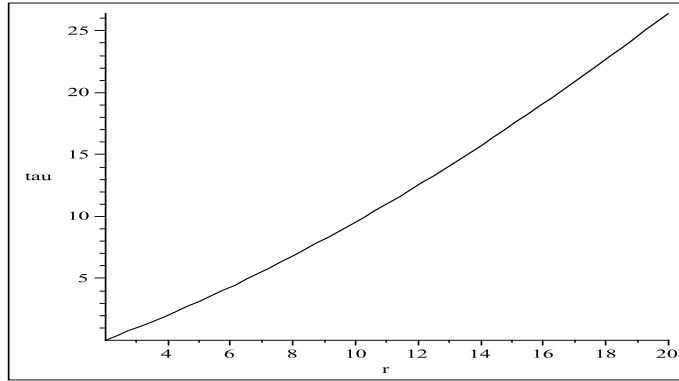


Figure 5. Radial geodesic, described in terms of τ , for a massive particle moving in a wormhole with $E = 1$, $M = 3$ and $\eta = 1$. The spatial infinities of each asymptotically flat regions are located at $r = 2$ and $r \rightarrow \infty$.

From Eqs. (12), (22) and (23), appropriately written for the radial case, we may obtain the expression which, after integration, gives r as a function of t .

$$t = \int \frac{E}{\sqrt{E^2 - (1 - 2\eta/r)^\lambda}} \frac{dr}{(1 - 2\eta/r)^\lambda} \quad (25)$$

Even with this simplification, as in the case with τ , we cannot integrate (25) to find an analytic expression of t as a function of r . The best one can do is finding a numerical solution for the integral. We did that for both cases of the naked singularities and wormholes.

Naked singularities In this case, we integrated (25) for many different values of E , M and η . We chose values of M and η compatibles with naked singularities. Qualitatively, the geodesics behave very much like the description in terms of τ . For $E \geq 1$ and $E < 1$, t goes to zero when $r \rightarrow 2\eta$. For $E \geq 1$, when r is large, r tends to a linear function of t . For $E < 1$, the geodesics do not extend to large values of r . As we have mentioned above, since the potential is the same as in the description in terms of τ , the turning points are also the same. Nevertheless, there is a quantitative difference between the two descriptions. We observe that, although, in both descriptions r is an increasing function of the time variable, it grows slower with t than with τ . The specific difference in the rate of growth between the two descriptions depends on the values of the parameters M and η . Here, we may, also, conclude that it always takes a finite time coordinate interval to travel from any finite value of r to the singularity located at $r = 2\eta$ and there is not an infinity potential wall near the naked singularity and the massive particles can reach it.

Wormholes In this case, we integrated (25) for many different values of E , M and η . We chose values of M and η compatibles with wormholes. In analogy with the case where the geodesics are described by τ , for $E \geq 1$, when r is large, r tends to a linear

function of t . On the other hand, for $E < 1$ they do not extend to large values of r . As we have mentioned above, since the potential is the same as in the description in terms of τ , the turning points are also the same. We found, here, some differences with respect to the description in terms of τ . The most important is that, for any value of E , the geodesics are not well behaved when $r \rightarrow 2\eta_+$. In fact, t goes to $-\infty$ in that limit. As another difference, we observe that, although, in both descriptions r is an increasing function of the time variable, it grows slower with t than with τ . The specific difference in the rate of growth between the two descriptions depends on the values of the parameters M and η . Due to the divergence in t when $r \rightarrow 2\eta_+$, we conclude, here, that it always takes an infinite time coordinate interval to travel from any finite value of r to the spatial infinity located at $r = 2\eta$. In the Figure 6, we show as an example a geodesic for the case: $E = 1$, $M = 3$ and $\eta = 1$. The spatial infinities of each asymptotically flat regions are located at $r = 2$ and $r \rightarrow \infty$ and the geodesics extends to large values of r .

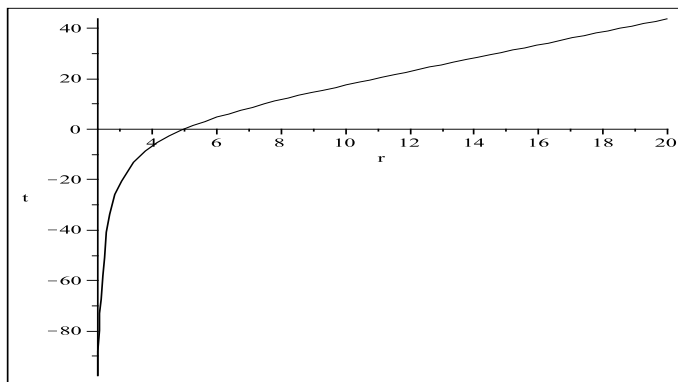


Figure 6. Radial geodesic, described in terms of t , for a massive particle moving in a wormhole with $E = 1$, $M = 3$ and $\eta = 1$. The spatial infinities of each asymptotically flat regions are located at $r = 2$ and $r \rightarrow \infty$.

4. Null Geodesics

4.1. Effective Potential

The null geodesics for the Wyman solution are derived almost in the same way the timelike geodesics were derived in the previous section. The only difference is that, here, the null line element contributes a different additional equation to the four geodesic equations. The new equation reads: $ds^2/d\chi^2 = 0$, where χ is the affine parameter used in the present case. Therefore, proceeding exactly as in the previous section we obtain the following effective potential equation,

$$\left(\frac{dr}{d\chi}\right)^2 + V(r)^2 = \frac{1}{b^2}, \quad (26)$$

where

$$V(r)^2 = r^{-2} \left(1 - \frac{2\eta}{r}\right)^{\frac{2M}{\eta} - 1} \quad (27)$$

and $b \equiv L/E$ is the photon impact parameter. $V(r)^2$ (27) is the effective potential for the motion of the photon in Wyman geometry.

$V(r)^2$ (27) has only one extreme point at $r = 2M + \eta$. Due to the domain of r it can only exist if $2M > \eta$ or $\lambda > 1/2$ and when it exists it is a maximum point. Therefore, we have three different cases: (i) $\lambda > 1/2$, the effective potential has a maximum point at $r = 2M + \eta$ and goes to zero at $r = 2\eta$; (ii) $\lambda = 1/2$, the effective potential has no extreme points and diverges to ∞ as $r \rightarrow 0$; (iii) $\lambda < 1/2$, the effective potential has no extreme points and diverges to ∞ as $r \rightarrow 2\eta$.

As we saw in Sec. 2, naked singularities and wormholes are characterized by certain subdomains of λ . Therefore, based on the above result, we may draw the effective potentials for naked singularities and wormholes. From these effective potentials, we shall be able to describe qualitatively the different orbits of photons.

4.2. Effective Potential for Naked Singularities

As it was mentioned in Subsec. 3.2, we are only concerned, here, with the class of ordinary naked singularities characterized $0 < \lambda < 1/2$. For this class, $V(r)^2$ (12) assumes the following values when $r \rightarrow 2\eta_+$ and $r \rightarrow +\infty$,

$$\lim_{r \rightarrow 2\eta_+} V(r)^2 = \infty, \quad \lim_{r \rightarrow +\infty} V(r)^2 = 0. \quad (28)$$

$V(r)^2$ (27) has no extreme points. In this case, whatever the impact parameter b the photons come in from infinity get reflected by the infinity potential wall near the naked singularity and return to infinity without ever reach the naked singularity.

Let us consider, as an example, the case where $M = 0.3$, $\eta = 1$ and $\lambda = 0.3$. In the Figure 7, we plot the effective potential diagram from $V(r)^2$ (27), for these parameter values. The naked singularity is located at $r = 2$.

4.3. Effective Potential for Wormholes

As it was mentioned in Subsec. 3.3, we are only concerned, here, with the class of ordinary wormholes characterized by $2 < \lambda < \infty$. In the spatial infinity of each asymptotically flat region the effective potential $V(r)^2$ (27) assumes the following values,

$$\lim_{r \rightarrow 2\eta_+} V(r)^2 = 0, \quad \lim_{r \rightarrow \infty} V(r)^2 = 0. \quad (29)$$

$V(r)^2$ (27) has a maximum point located at $r = 2M + \eta$. In this point the photons have unstable circular orbits. For sufficiently small impact parameter b the photons may travel from one asymptotically flat region to the other. Otherwise, they come in from spatial infinity of an asymptotically flat region get reflected by the effective potential and return to spatial infinity in the same asymptotically flat region.

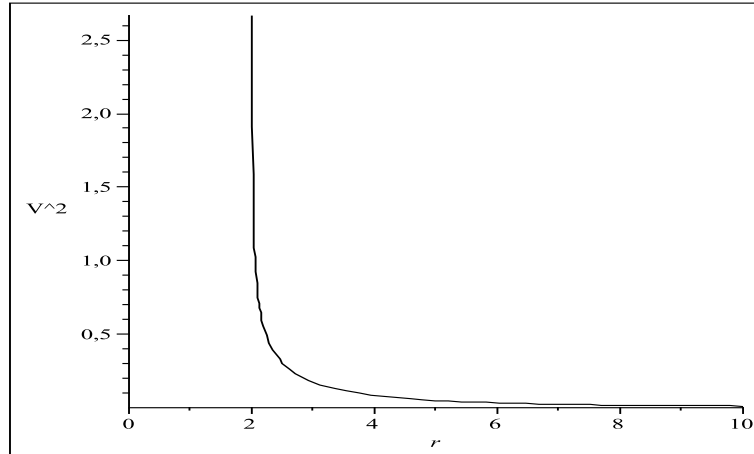


Figure 7. Effective potential diagram from $V(r)^2$ (27), for photons moving in a naked singularity with $M = 0.3$, $\eta = 1$ and $\lambda = 0.3$. The naked singularity is located at $r = 2$.

Let us consider, as an example, the case where $M = 30$, $\eta = 1$ and $\lambda = 30$. In the Figure 8, we plot the effective potential diagram from $V(r)^2$ (27), for these parameter values. The spatial infinities of each asymptotically flat regions are located at $r = 2$ and $r \rightarrow \infty$.

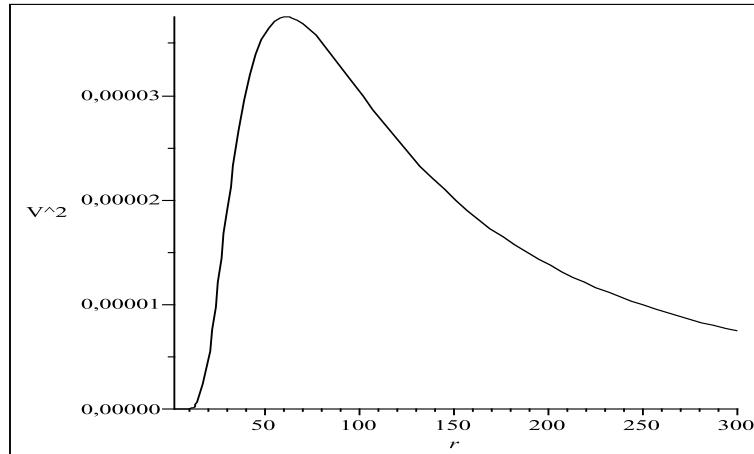


Figure 8. Effective potential diagram from $V(r)^2$ (27), for photons moving in a wormhole with $M = 30$, $\eta = 1$ and $\lambda = 30$. The spatial infinities of each asymptotically flat regions are located at $r = 2$ and $r \rightarrow \infty$.

4.4. Radial null geodesics

4.4.1. Description in terms of χ The description of the null geodesics in terms of the affine parameter χ is trivial, when we consider radial geodesics ($\dot{\theta} = \dot{\phi} = L = 0$). That is the case because the effective potential equation for the radial motion of photons reduces to $(dr/d\chi)^2 = E^2$. It means that the effective potential is zero and the photons move freely following straight lines: $r = \pm E\chi + q$, where q is an integration constant

and the + and – signs mean, respectively, outgoing and ingoing geodesics. This result is valid for photons moving in the naked singularity as well as in the wormhole geometries.

4.4.2. Description in terms of t The description of the null geodesics in terms of the time coordinate t may be derived with the aid of (10), appropriately written in terms of χ , and the equation $(dr/d\chi)^2 = E^2$. Then, we have: $(dt/dr)^2 = (dt/d\chi)^2/(dr/d\chi)^2 = (1 - 2\eta/r)^{-2\lambda}$. From this equation, we obtain t as a function of r after performing the following integral,

$$t = \pm \int \left(1 - \frac{2\eta}{r}\right)^{-\lambda} dr \quad (30)$$

Fortunately, we can analytically integrate (30) to find,

$$t = \pm \left[r + 2M \ln\left(\frac{r}{2\eta}\right) - \frac{2M(M + \eta)}{r} {}_3F_2\left(\frac{M}{\eta} + 2, 1, 1; 2, 3; \frac{2\eta}{r}\right) \right] + Q. \quad (31)$$

where the + and – signs mean, respectively, outgoing and ingoing geodesics. Q is an integration constant and F is an hypergeometric function. If we introduce the condition $M = \eta$ in (31), we obtain: $t = r + 2M \ln(r - 2M) + Q$, where Q is an integration constant. That expression is the well-known radial, outgoing null geodesics for the Schwarzschild geometry parametrized by the time coordinate [1].

For large values of r (31) indicates that r becomes a linear function of t , for both naked singularities and wormholes. On the other hand, a great difference appears between naked singularities and wormholes in the limit when $r \rightarrow 2\eta_+$. Observing (31), we see that the limit of t when $r \rightarrow 2\eta_+$ depends crucially on the behaviour of ${}_3F_2$ when $r \rightarrow 2\eta_+$. From the theorem 2.1.2, page 62 in [20], we learn that in the limit $r \rightarrow 2\eta_+$, ${}_3F_2(M/\eta + 2, 1, 1; 2, 3; 2\eta/r)$ converges absolutely if $M/\eta < 1$ and diverges otherwise ($M/\eta \geq 1$). Therefore, for naked singularities t will converge for a finite value and for wormholes it will diverge to $-\infty$. It is actually possible to compute the limit of ${}_3F_2(M/\eta + 2, 1, 1; 2, 3; 2\eta/r)$ when $r \rightarrow 2\eta_+$. In order to do that, we must use: equation (2.2.2), page 67 in [20], ${}_2F_1(1, 1; 2; z) = -\frac{1}{z} \ln|1 - z|$ and $\Gamma(x)\Gamma(1 - x) = \pi/\sin(\pi x)$. After an integration we find the following result,

$${}_3F_2(\lambda + 2, 1, 1; 2, 3; 1) = \frac{2\eta}{M + \eta} \left[1 - \psi\left(1 - \frac{M}{\eta}\right) - \gamma \right], \quad (32)$$

where $\psi(x) \equiv \Gamma'(x)/\Gamma(x)$ is the digamma function, $\Gamma(x)$ is the gamma function and $\gamma = 0.5772156649\dots$ is the Euler constant. Therefore, introducing this result in (31) we obtain the value of t when $r \rightarrow 2\eta_+$,

$$\lim_{r \rightarrow 2\eta_+} t = 2(\eta - M) + 2M \left[\psi\left(1 - \frac{M}{\eta}\right) + \gamma \right] + Q. \quad (33)$$

Based on the above results, we may conclude that for the case of naked singularities it always takes a finite time coordinate interval to travel from any finite value of r to the singularity located at $r = 2\eta$. On the other hand, it always takes an infinite time

coordinate interval to travel from any finite value of r to the spatial infinity located at $r = 2\eta$, in the case of wormholes. Both results are qualitatively analogous to the corresponding ones found for the radial timelike geodesics. Finally, we notice, also, that for null radial geodesics there is not an infinity potential wall near the naked singularity and the photons can reach it.

5. Conclusions.

In the present work, we studied qualitative features of orbits of massive particles and photons moving in the naked singularity and wormhole spacetimes of the Wyman solution. These orbits are the timelike geodesics for massive particles and null geodesics for photons. Combining the four geodesic equations with an additional equation derived from the line element, we obtained an effective potential for the massive particles and a different effective potential for the photons. We investigated all possible types of orbits, for massive particles and photons, by studying the appropriate effective potential. We noticed that for certain values of $\sigma^2 > 0$, there is an infinity potential wall that prevents both massive particles and photons ever to reach the naked singularity. This result is similar to the one found in [4] for timelike geodesics of the naked singularity present in the Reissner-Nordström spacetime. We noticed, also, that for certain values of $-M_0^2 \leq \sigma^2 < 0$, the potential is finite everywhere, which allows massive particles and photons moving from one wormhole asymptotically flat region to the other. We also computed the radial timelike and null geodesics for massive particles and photons, respectively, moving in the naked singularities and wormholes spacetimes.

Acknowledgments

G. Oliveira-Neto thanks CNPq and FAPERJ for partial financial support and G. F. Sousa thanks CAPES for financial support.

References

- [1] For a detailed explanation see: Misner C W, Thorne K S and Wheeler J A 1973 *Gravitation* (New York: Freeman)
- [2] Jaklitsch M J, Hellaby C and Matravers D R 1989 *Gen. Rel. Grav.* **21** 941; Stuchlík Z and Calvani M 1991 *Gen. Rel. Grav.* **23** 507; Stuchlík Z and Hledík S 1999 *Phys. Rev. D* **60** 044006; Podolský J 1999 *Gen. Rel. Grav.* **31** 1703; Kraniotis G V and Whitehouse S B 2003 *Class. Quantum Grav.* **20** 4817; Kraniotis G V 2004 *Class. Quantum Grav.* **21** 4743; Cruz N, Olivares M and Villanueva J R 2005 *Class. Quantum Grav.* **22** 1167
- [3] Cohen J M and Gautreau R 1979 *Phys. Rev. D* **19** 2273; Stuchlík Z and Hledík S 2000 *Class. Quantum Grav.* **17** 4541; Stuchlík Z and Slaný P 2004 *Phys. Rev. D* **69** 064001
- [4] Qadir A and Siddiqui A A 2007 *Int. J. Mod. Phys. D* **16** 25
- [5] Graves J C and Brill D R 1960 *Phys. Rev.* **120** 1507; Azreg-Ainou M and Clément G 1990 *Gen. Rel. Grav.* **22** 1119
- [6] Wyman M 1981 *Phys. Rev. D* **24** 839

- [7] Fisher I Z 1948 *Zh. Eksp. Teor. Fiz.* **18** 636 and an English version available in gr-qc/9911008; Bergman O and Leipnik R 1957 *Phys. Rev.* **107** 1157; Buchdahl H A 1959 *Phys. Rev.* bf 111 1417; Janis A I, Newman E T and Winicour J 1968 *PRL* **20** 878; Chase J E 1970 *Commun. Math. Phys.* bf 19 276; Agnese A G and LaCamera M 1982 *Lett. Nuovo Cimento* **35** 365; Agnese A G and LaCamera M 1985 *Phys. Rev. D* **31** 1280; Dionysion D D 1982 *Astro. Space Sci.* **83** 493; Froyland J 1982 *Phys. Rev. D* **25** 1470; Roberts M D 1985 *Gen. Rel. Grav.* **17** 913; Roberts M D 1985 *Class. Quantum Grav.* **2** L69; Roberts M D 1988 *Astro. Space Sci.* **147** 321
- [8] Roberts M D 1989 *Gen. Rel. Grav.* **21** 907
- [9] Jetzer P and Scialom D 1992 *Phys. Lett. A* **169** 12
- [10] Clayton M A, Demopoulos L and Legare J 1998 *Phys. Lett. A* **248** 131
- [11] Oliveira-Neto G and Takakura F I 2005 *J. Math. Phys.* **46** 062503
- [12] Brady P R 1994 *Class. Quantum Grav.* **11** 1255
- [13] Oshiro Y, Nakamura K and Tomimatsu A 1994 *Prog. Theor. Phys.* **91** 1265
- [14] Choptuik M W 1993 *Phys. Rev. Lett.* **70** 9
- [15] Christodoulou D 1986 *Commun. Math. Phys.* **105** 337; Christodoulou D 1986 *Commun. Math. Phys.* **106** 587; Christodoulou D 1987 *Commun. Math. Phys.* **109** 591; Christodoulou D 1987 *Commun. Math. Phys.* **109** 613; Christodoulou D 1991 *Commun. Pure Appl. Math.* **XLIV** 339; Christodoulou D 1993 *Commun. Pure Appl. Math.* **XLVI** 1131; Christodoulou D 1994 *Ann. Math.* **140** 607
- [16] Yilmaz H 1958 *Phys. Rev.* **111** 1417; Rosen N 1970 *Proc. Int. Conf. on Relativity (Cincinnati)* ed Carmeli *et al* (New York: Plenum Press) 229
- [17] Hayward S A, Kim S W and Lee H 2002 *Phys. Rev. D* **65** 064003
- [18] Morris M S and Thorne K S 1988 *Am. J. Phys.* **56** 395
- [19] D'Inverno R A 1992 *Introducing Einstein's Relativity* (Oxford: Oxford University Press)
- [20] Andrews G E, Askey R and Roy R 1999 *Special Functions* (Cambridge: Cambridge University Press)